

# Crystallization of nanocomposites of an isotactic random butene-1/ethylene copolymer and layered double hydroxide

Ayret Mollova<sup>1</sup>, Igor Kolesov<sup>1</sup>, René Androsch<sup>1,\*</sup>, Johan Labuschagne<sup>2</sup>, Walter Focke<sup>2</sup> and Sergio S. Funari<sup>3</sup>

<sup>1</sup>Center of Engineering Sciences, Martin-Luther-University Halle-Wittenberg, 06099 Halle/Saale, Germany

<sup>2</sup>Department of Chemical Engineering, University of Pretoria, Pretoria 0028, South Africa

<sup>3</sup>Hasylab at DESY, Notkestrasse 85, 22607 Hamburg, Germany

\*Correspondence author: R. Androsch. e-mail: rene.androsch@iw.uni-halle.de

## Abstract

The effect of the presence of a layered double hydroxide (LDH) nanofiller on the crystallization behavior of a random isotactic butene-1/ethylene copolymer was investigated. Addition of LDH enhanced heterogeneous nucleation of the ordering process of the polymer matrix leading to an increase of the temperature of formation of the Form II mesophase on cooling the melt. Consequently, the size of spherulites of the polymer matrix was markedly reduced in the nanocomposites. In contrast, the Form II mesophase–Form I crystal phase transition kinetics and the final crystallinity were not affected by the presence of LDH. Addition of the LDH nanofiller led to a beneficial increase of the stiffness which suggests a route for compensating of the lower stiffness of the random copolymer compared to the homopolymer. Random copolymerization accelerates the disadvantageous room-temperature mesophase–crystal transition, but results in a reduction of the crystallinity. The addition of LDH counterbalances the lowering of the crystal fraction.

## Introduction

Isotactic polybutene-1 (iPB-1) is a semicrystalline polymer with a crystallinity of 50–70 %. Crystallization of iPB-1 on supercooling the melt is a multi-stage process, involving in a first step the formation of an unstable tetragonal mesophase (Form II) on cooling, which then slowly transforms to stable trigonal crystals (Form I) during storage of the material at ambient temperature. The mesophase–crystal phase transition is fastest at about room temperature, and requires at this condition a period of about 2 weeks. The change of the crystal structure is associated with a reduction of the specific volume of the ordered phase by 5 %, and leads to macroscopic shrinkage, internal stress, and a drastic change of properties. The melting temperature increases by 10–20 K, the hardness, stiffness and strength increase, but the ductility decreases. This time-dependence of the physical properties impacts the end-use performance. Since it restricts the engineering potential of this important polymeric material, there is a need to control the specific mesophase/crystal polymorphism such that short-term aging after processing is minimized [1–5].

The kinetics of the mesophase–crystal phase transition can be controlled by varying the crystallization conditions and, more effectively, by variation of the molecular structure. An advantageous route for acceleration of the iPB-1 mesophase–crystal transition is the insertion of constitutional defects into the butene-1 chain [6–9]. Early research in this field was published by Turner-Jones [6] and Gianotti [7]. Turner-Jones showed that random copolymerization of butene-1 with 1-hexene, 1-octene or 4-methylpentene delays the mesophase–crystal phase transition and even stabilizes the mesophase. Ethylene, propylene or 1-pentene co-units, in contrast, accelerate the mesophase–crystal transition. When added at sufficiently high levels, they even allow direct formation of metastable crystals from the supercooled melt. Quantitative analysis of the solidification kinetics of random copolymers based on butene-1 showed that addition of 5 m% ethylene reduced the half-time of the mesophase–crystal transition from 170 h in the homopolymer to only 3.5 h [8]. Recent evaluation of the crystallization behavior of the copolymer system butene-1/propylene suggested even direct formation of Form I crystals from the melt if the butene-1 concentration is set between 60 and 80 % [9].

While random copolymerization of butene-1 with ethylene or propylene leads to acceleration of the mesophase–crystal transition at room temperature, there are concomitant changes of structure and ultimate properties. In general, random copolymerization is considered as an effective tool to tailor the process of melt-crystallization. Besides reduction of the crystallization rate and temperature of crystallization, the degree of crystallinity is lowered, and crystals and spherulites typically are less perfect and smaller than in the corresponding homopolymer. Such effects are often sought to fit specific application requirements. However, when using random copolymerization to tailor the phase transition kinetics of iPB-1, the resulting reduction of the crystallinity may be considered disadvantageous. According to the mixing rules for the prediction of properties of multi-phase materials [10–13], the decrease of the crystallinity is accompanied by corresponding changes of ultimate properties such as stiffness, strength or hardness.

The specific objective of this work was to target compensation of the loss of stiffness in iPB-1 due to random copolymerization that leads to a reduction of crystallinity. We follow the idea that the disadvantageous loss of the perfection of crystals and the decrease of the degree of crystallinity in random iPB-1 copolymers, which results in lower stiffness, reduced strength, and lower thermal stability, can be countered by the addition of low amounts of suitable nanofiller. This strategy retains the advantageous effects offered by increased ductility/impact strength due to reduced crystallinity and accelerated room-temperature phase transformation following melt-processing.

Prior research in the field of iPB-1 nanocomposites includes modification with montmorillonite (MMT) [14–17]. In earlier work it has been shown that melt-processing leads to beneficial intercalation of iPB-1 molecules into MMT galleries, minor acceleration of the mesophase–crystal transition, and distinct increase of properties such as the storage modulus [14, 15]. MMT, even if not exfoliated, was found to disrupt the ordered morphology of unmodified iPB-1, to nucleate the ordering process, and to significantly affect the mechanical property profile. For example, addition of 5 m% organo-modified MMT led to a doubling of the modulus, while the elongation at break and impact resistance were drastically decreased [16].

Little research has been performed using layered double hydroxides (LDH) as nanofiller in iPB-1 [18], despite specific advantages like synthetic production, compliance with EU regulations for contact with foodstuffs, relatively high temperature stability, and good compatibility with rather non-polar polyolefins [19–21]. Earlier investigations focused on the analysis of the effect of addition of Perkalite LDH to iPB-1 on the mesophase–crystal transition rate. It was assumed that nanofillers impose stress on the primarily formed mesophase of iPB-1, which is known to accelerate the subsequent mesophase–crystal transition [22, 23].

In contrast to the above described approach of using nanofillers to accelerate the mesophase–crystal transition of iPB-1, we follow the route to increase the transition rate by random copolymerization, and to use LDH nanofillers to re-adjust the level of thermo-mechanical properties of the polymer matrix. In this initial study, we used a specific butene-1/ethylene random copolymer which in the past was analyzed with regard to the solidification kinetics [8, 24] and effect of the mesophase–crystal transition on mechanical properties in blends with low-density polyethylene [24]. Nanocomposites were prepared by melt-mixing, with the dispersion of LDH in the polymer matrix subsequently analyzed by transmission electron microscopy. The effect of LDH on the crystallization behavior of the polymer matrix was evaluated by calorimetry, polarizing optical microscopy, and X-ray diffraction, while the reinforcing effect was judged by measurement of the modulus of elasticity.

## Experimental

### Materials and preparation

In the present work, we employed a Ziegler–Natta catalyst synthesized butene-1/ethylene random copolymer (iPB-Eth) from Basell Polyolefins (Germany) with a melt-flow index of  $1 \text{ g (10 min)}^{-1}$  (503 K, 2.16 kg), containing 0.75 m% ethylene [8]. The mass-average molar mass is 470 kDa, and the fraction of isotactic pentads is 87.6 % [8]. The layered double hydroxide was Hydrotalcite grade Pyrosorb, supplied by Nkomazi Chemicals (Pty) Ltd. (South Africa). This material had the approximate composition  $[\text{Mg}_{0.66}\text{Al}_{0.34}(\text{OH})_2](\text{CO}_3)_{0.17} \cdot \frac{1}{2}\text{H}_2\text{O}$ . Nanocomposites containing 5 and 10 m% LDH, iPB-Eth/LDH-5 and iPB-Eth/LDH-10, respectively, were prepared using a Haake MiniLab II Micro Rheology Compounder, operated at 50 rpm and 160 °C. The extrudates were further processed to films of about 250  $\mu\text{m}$  thickness by compression-molding using a Perkin-Elmer FTIR press with a Lot-Oriel/Specac film maker die and heating accessory. The unmodified polymer was subjected to an identical processing history.

### Instrumentation

#### Transmission electron microscopy

Transmission electron microscopy (TEM) was employed to obtain information about the degree of deagglomeration of primary LDH particles, about intercalation of polymer segments in between hydroxide layers, and/or eventual exfoliation of the latter. Ultrathin sections with a thickness between 80 and 200 nm were prepared using a Reichert Ultramicrotome Ultracut E equipped with a Diatome diamond knife. The sections were placed on a copper 300 mesh grid and then investigated using a Jeol JEM-2100F TEM, operated at 200 kV.

### Differential scanning calorimetry

Differential scanning calorimetry (DSC) data were collected for analysis of the temperature of crystallization of the polymer matrix in absence and presence of the LDH nanofiller. A heat-flux DSC 820 from Mettler-Toledo was used. It was equipped with a liquid nitrogen accessory for controlled cooling, with the temperature and heat-flow-rate signals of the instrument calibrated as described in text books [25]. The cooling experiments were performed at a rate of 5 K min<sup>-1</sup>, and using nitrogen as purge gas.

### Polarizing optical microscopy

Polarizing optical microscopy (POM) was employed to gain knowledge about the effect of LDH on the final spherulitic superstructure of the semicrystalline polymer matrix. Specimens were prepared by melting between Plano microscope cover slips using a hot stage. The specimens were then placed in a Mettler-Toledo microscope hot stage FP84 HT connected to an FP90 controller, melted by heating to 423 K, and finally cooled to 393 K and ambient temperature at rates of 10 and 2 K min<sup>-1</sup>, respectively. During cooling from 393 to 298 K at 2 K min<sup>-1</sup>, images were captured each 30 s using a Moticam 2300 CCD camera, to obtain information about the crystallization temperature. We used a Motic BA410 microscope.

### Wide-angle X-ray scattering

Temperature-resolved wide-angle X-ray scattering (WAXS) data were measured at the A2 SAXS/WAXS beamline at HASYLAB/DESY (Germany), to obtain information about the kinetics of mesophase formation on cooling the unmodified and nanofiller modified iPB-1-based copolymer. The wavelength of the radiation was 0.15 nm and the sample-detector distance was about 140 mm. Scattering data were collected in transmission mode with a two-dimensional MarCCD165 detector. Several layers of polymer film were wrapped into aluminum foil, and placed in a temperature-controlled sample holder. The normal of the sample film was oriented parallel to the beam with a size of about 2 mm (vertical direction) × 3 mm (horizontal direction). Samples were heated in vacuum atmosphere to 423 K, kept at this temperature for 3 min, and then cooled at 5 K min<sup>-1</sup>. X-ray frames were acquired each 30 s, and allowed in situ observation of the formation of mesophase. WAXS data were additionally collected during aging at room temperature to gain information about the effect of LDH on the mesophase–crystal transition kinetics of the polymer matrix, the final crystal structure, and the degree of crystallinity. We used an URD 63 diffractometer from Seifert-FPM, using Ni-filtered Cu K<sub>α</sub> radiation with a wavelength of 0.15418 nm. The instrument was operated in transmission mode, with the scattered intensity recorded using a scintillation counter.

### Dynamic mechanical analysis

Dynamic mechanical analysis (DMA) experiments were performed in tensile mode using the Mark III measuring head from Rheometric Scientific, for measurement of the stiffness of the sample film of different LDH content. The cross-section of the samples and the distance between the clamps were 0.25 × 4.5 mm<sup>2</sup> and 12 mm, respectively. The strain was modulated with an amplitude of 0.05 % at a frequency of 1 Hz. The temperature was kept constant 300 K. Data presented are averages of three independent measurements.

## Results and discussion

### TEM structure

In Fig. 1 TEM images of the system iPB-Eth/LDH-10 at different magnifications are presented. The images are also representative for the system iPB-Eth/LDH-5. The micrographs provide information about the degree of deagglomeration of clusters of primary LDH particles, their disintegration and partially achieved separation of hydroxide layers. Optical microscopy revealed that the present mixing scheme resulted in the formation of a mixed micro-nanocomposite morphology. Clusters of LDH particles as large as several micrometers in size are observed. The left and center images of Fig. 1 show the presence of disintegrated clusters and sub-micrometer particles but also isolated stacks of hydroxide layers with a lateral dimension of about 200 nm and thickness of few nanometers. The long period of the LDH galleries, that is, the repeating period in the stacks of alternating metal hydroxide and anion layers, according to X-ray measurements, was around 0.75 nm. We assume therefore that complete exfoliation of the hydroxide layers was not achieved. Since the platelet shown in the right image of Fig. 1 may be inclined and not viewed edge-on, final conclusions about the degree of exfoliation may not be drawn. Though a uniform size of LDH particles of less than 1  $\mu\text{m}$  has not been achieved with the used preparation scheme, we still classify the samples as partial nanocomposites since there are throughout and reproducibly observed LDH platelets with a thickness less than 100 nm.

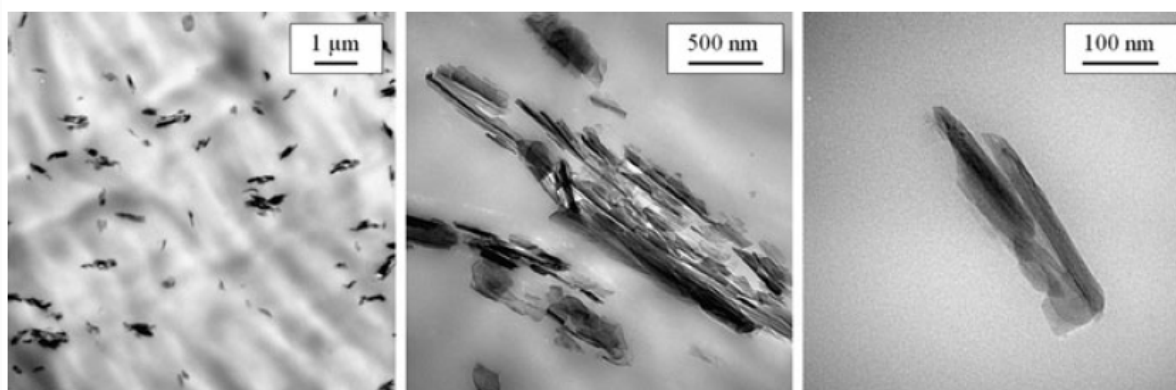


**Fig. 1** TEM structure of the nanocomposite iPB-Eth/LDH-10 at different magnification

### Primary crystallization of the polymer matrix

Figure 2 shows a series of POM micrographs recorded during cooling the melt of iPB-Eth/LDH-0 (left), iPB-Eth/LDH-5 (center), and iPB-Eth/LDH-10 (right) at a rate of 2 K  $\text{min}^{-1}$  from 393 and 303 K. The experiment was performed to gain knowledge about the temperature of crystallization ( $T_c$ ) and the spherulitic superstructure of the polymer matrix in the various nanocomposites. Each set of micrographs consists of 90 images, to be read from top to bottom, starting with the left of the three columns. The crystallization temperatures of the investigated samples are indicated with the white circle, followed by a vertical arrow. In case of the unmodified copolymer, the crystallization temperature is around 344 K, while in case of the nanocomposites containing 5 and 10 m% LDH, the crystallization temperatures are increased to 349 and 352 K, respectively. Obviously, the LDH filler nucleates the ordering process of the polymer matrix, and increases the gross crystallization rate.

The primary crystallization process, as is judged by completion of the spherulite growth is finished at the particular cooling condition at 328, 335, and 345 K, in the various samples containing 0, 5, and 10 m% LDH, respectively.

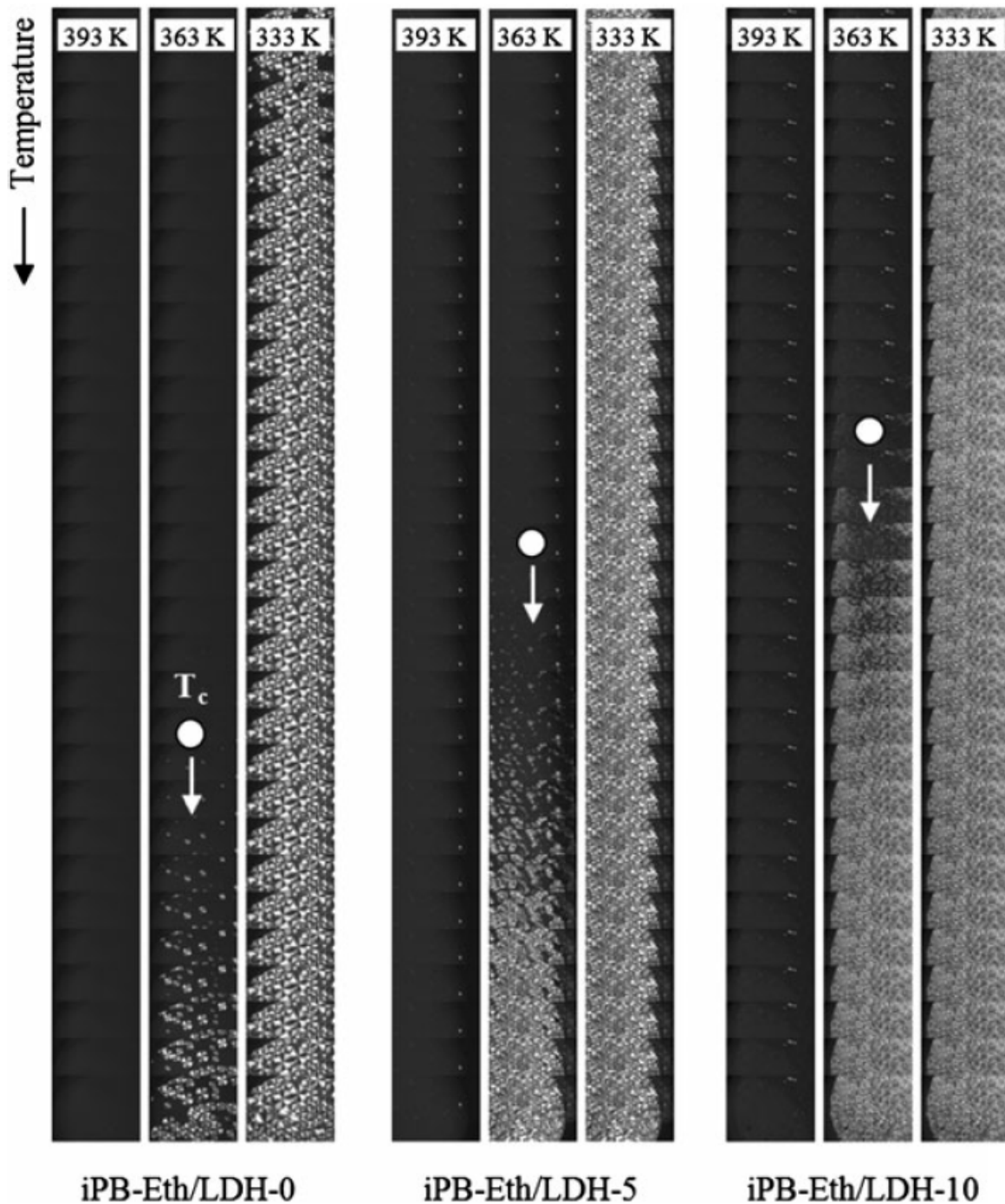


**Fig. 2** Series of POM micrographs recorded during continuous cooling the melt of iPB-Eth/LDH-0 (*left*), iPB-Eth/LDH-5 (*center*), and iPB-Eth/LDH-10 (*right*) at a rate of  $2 \text{ K min}^{-1}$  from 393 and 303 K. The *top left image* of each series was taken at 393 K, and represents the start of the cooling experiment. The images need to be read from *top to bottom*, starting with the *left column*. The *white circles* indicate the onset of crystallization

The assumption of a nucleating effect of the LDH particles on the polymer crystallization process is supported by the observation of an increased number/lower size of spherulites in samples containing LDH. In Fig. 3, POM micrographs of iPB-Eth/LDH-0, iPB-Eth/LDH-5, and iPB-Eth/LDH-10, which were taken at room temperature after completion of the cooling experiment of Fig. 2, are shown.

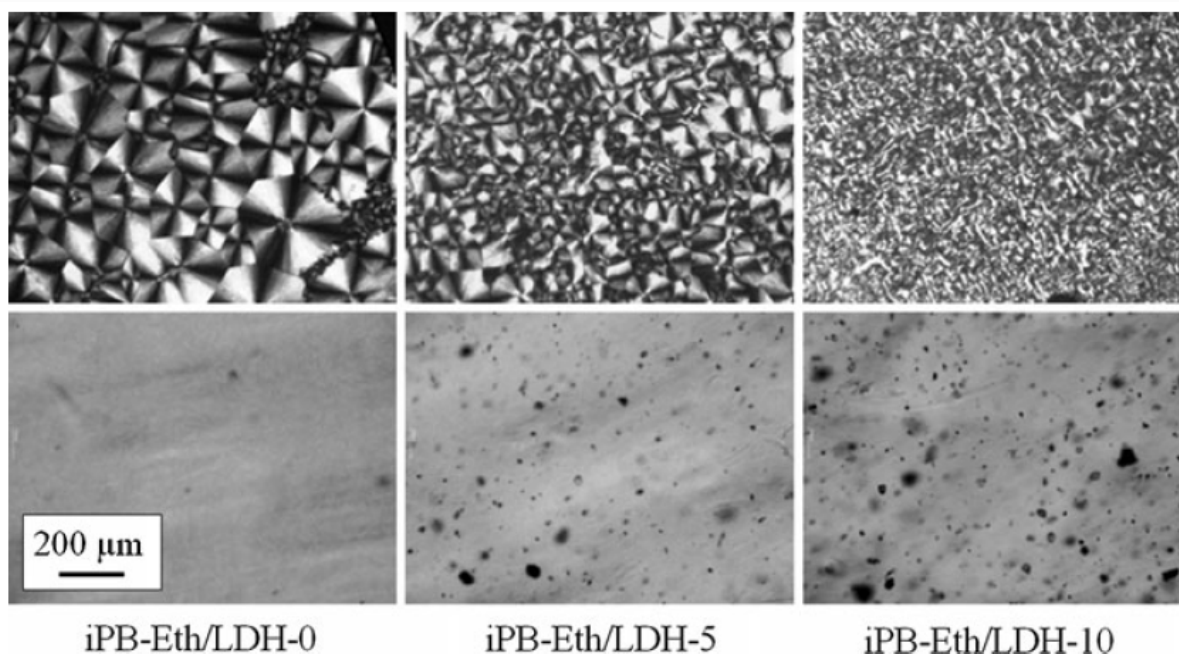


**Fig. 3** POM micrographs of iPB-Eth/LDH-0 (*left*), iPB-Eth/LDH-5 (*center*), and iPB-Eth/LDH-10 (*right*), taken at room temperature after completion of the cooling experiment of Fig. 2. The *top-row images* were collected with the samples placed between crossed polarizers while the *bottom-row images* were collected in absence of polarizers

The top-row shows images with the samples placed between crossed polarizers, while the bottom images were collected in absence of polarizers. In case of the unmodified polymer iPB-Eth/LDH-0 (left images), rather large and perfect spherulites with a size around 100  $\mu\text{m}$  were formed during cooling. In case of nanocomposites with 5 and 10 m% LDH (center and right images), the spherulites are reduced in size, and the rather perfect radial symmetry, as is seen with the Maltese cross in the unmodified polymer, is lost. The bottom images, taken in plain transmission mode without using polarizers, serve as an addendum to the TEM images of Fig. 1. They show the LDH distribution at the micrometer length scale. It can clearly be seen that besides presence of nanometer size LDH platelet stacks, as shown with the right image in Fig. 1, non-disintegrated clusters of LDH particles, several tenths of micrometer in size, remained after the specific melt-mixing route used presently.

Figure 4 shows the DSC cooling scans of iPB-Eth/LDH-0 (bottom curve), iPB-Eth/LDH-5 (center curve), and iPB-Eth/LDH-10 (top curve) recorded using a rate of temperature change of 5 K  $\text{min}^{-1}$ . Visual inspection of the data, and as is emphasized with the arrows, revealed that addition of LDH led to an increase of the temperature of mesophase formation. In addition it appears that the peak width was decreasing on addition of LDH. Both observations prove that the nucleation rate and therefore overall crystallization/mesophase-formation rate was increased in the

nanocomposites compared to the unmodified iPB-Eth copolymer. Quantitative information about the onset temperature and enthalpy of the mesophase-formation process are provided at the right-hand side of each curve. The observed mesophase-formation onset temperatures are 337, 346, and 351 K for iPB-Eth/LDH-0, iPB-Eth/LDH-5, and iPB-Eth/LDH-10, respectively, which compare to 344, 349, and 352 K, measured by hot-stage microscopy. The minor difference of temperatures obtained by DSC and microscopy may be attributed to the different cooling rates applied; faster cooling is connected with a decrease of the temperature of the phase transition. Due to the nucleation effect of LDH in the nanocomposites, however, the cooling-rate effect on the phase transition temperature becomes negligible.

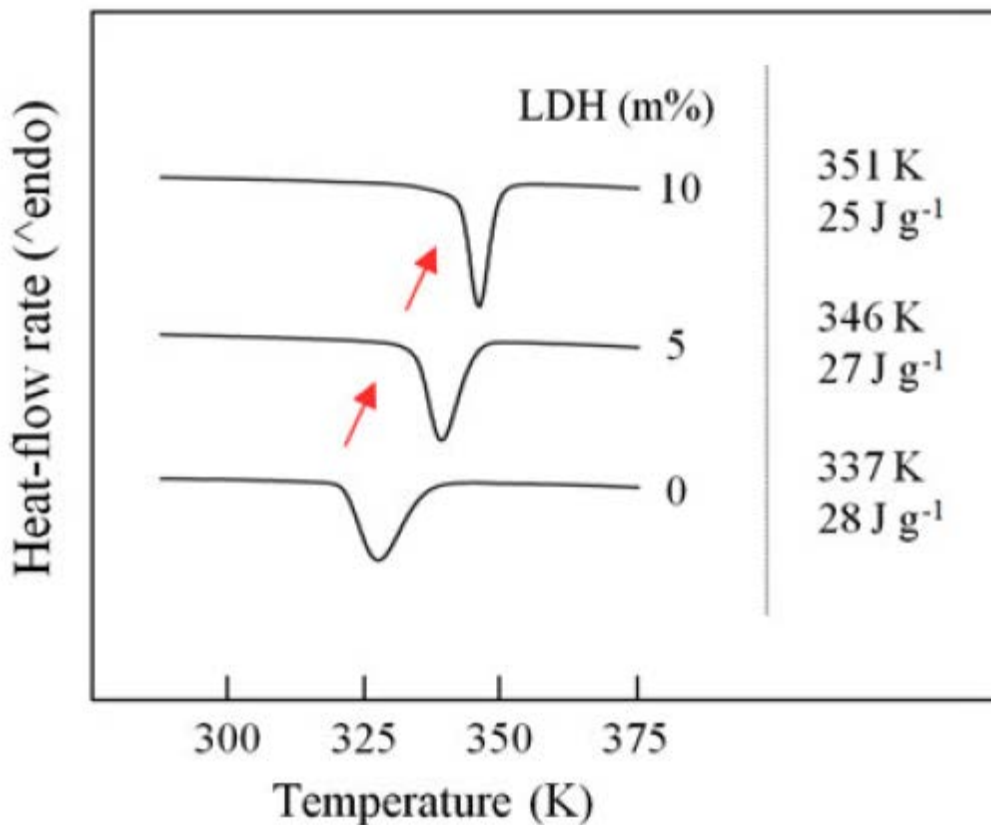


**Fig. 4** DSC cooling scans, heat-flow rate as a function of temperature, of iPB-Eth/LDH-0 (*bottom*), iPB-Eth/LDH-5 (*center*), and iPB-Eth/LDH-10 (*top*), recorded at 5 K min<sup>-1</sup>. At the *right-hand side* of each curve are provided information about the onset temperature and enthalpy of crystallization

The enthalpy of mesophase formation of the unmodified copolymer is 28 J g<sup>-1</sup>, and can be re-calculated to a phase fraction of about 45 % (=28 J g<sup>-1</sup>/62.5 J g<sup>-1</sup> × 100 %), with 62.5 J g<sup>-1</sup> being the bulk enthalpy of mesophase formation of iPB-1 [26]. Taking into account that the polymer fraction in the weighted DSC nanocomposite samples is lower than in the unmodified copolymer, the observed enthalpies of mesophase formation of 27 and 25 J g<sup>-1</sup> indicate an unchanged mesophase fraction in the polymer matrix of the nanocomposites.



### Mesophase/crystal polymorphism of the polymer matrix

In Fig. 5 WAXS curves of iPB-Eth/LDH-0 (bottom curve), iPB-Eth/LDH-5 (center curve), and iPB-Eth/LDH-10 (top curve), with the measurements performed after the samples have been aged for several weeks at ambient temperature are shown. In general, on cooling the melt of iPB-1, formation of mesophase is observed first, which subsequently transforms to crystals on aging. For the homopolymer it is known that the room-temperature mesophase–crystal transition may be completed after 1–2 weeks while in random copolymers, depending on the exact composition, the phase transition is accelerated. In case of the specific random copolymer used in the present work the mesophase–crystal transition ends prematurely after about 2–3 days [24].

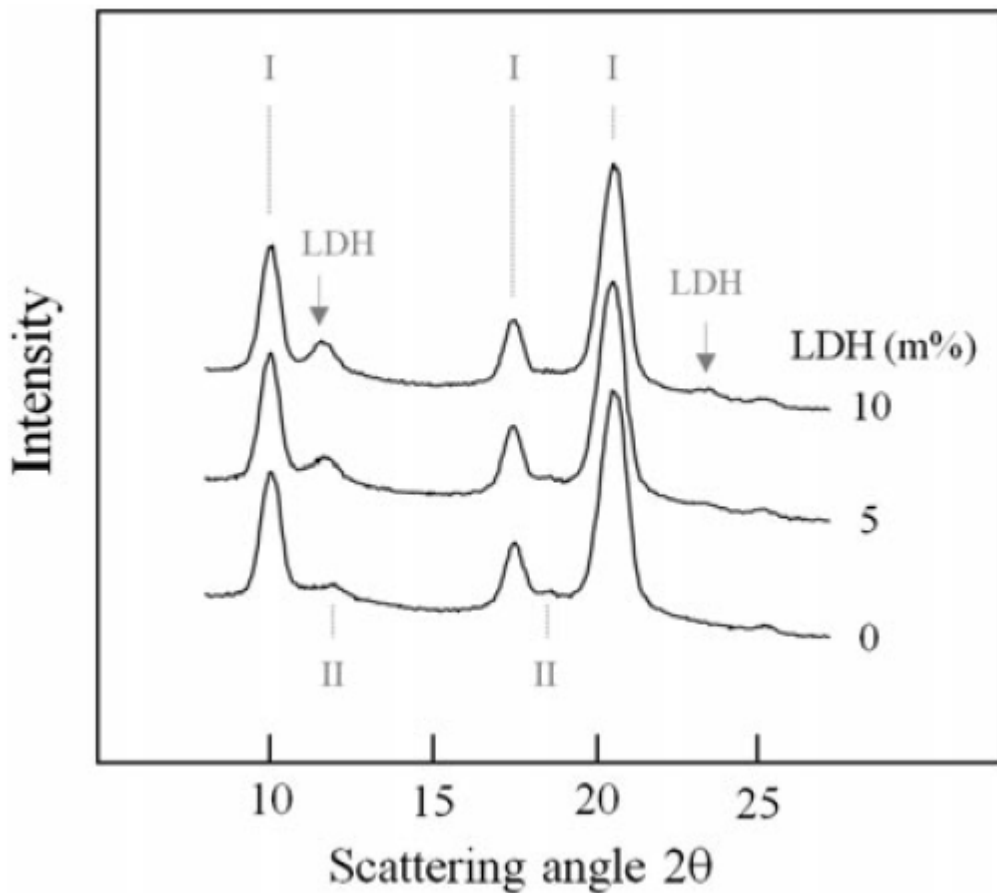


**Fig. 5** WAXS data, intensity as a function of scattering angle, of iPB-Eth/LDH-0 (bottom), iPB-Eth/LDH-5 (center), and iPB-Eth/LDH-10 (top), taken after extended aging of samples at room temperature

The data of Fig. 5 provide evidence that extended annealing of nanocomposites containing 5 and 10 m% LDH leads to similar final X-ray structure of the polymer matrix as is evident in case of the unmodified sample. The strong peaks at about 10.0, 17.5, and 20.3°  $2\theta$  indicate predominant presence of Form I crystals, while the weak peaks at 11.8 and 18.4 deg  $2\theta$  reveal minute amount of Form II mesophase, even after extended annealing. The presence of LDH in the nanocomposite is

detected with the peaks at  $11.6$  and  $23.5^\circ 2\theta$ , being proportional in intensity to its content in the samples. The crystallinity of the polymer matrix is not affected by the presence of LDH and amounts to about 65 % in all samples analyzed. Accordingly, it seems that there is a slight increase of the ordered phase during aging since DSC suggested an initial content of only 45 % mesophase after cooling.

Further knowledge about the mesophase/crystal polymorphism of the polymer matrix was gained by temperature- and time-resolved X-ray experiments. In Fig. 6, for illustration, a series of WAXS curves obtained on iPB-Eth/LDH-5 is shown. The sample was initially slowly cooled from the melt state, and then aged for several weeks at ambient temperature, before the start of the experiment. The data in Fig. 6 need to be read from bottom to top. First the aged sample was heated from 298 to 423 K. It was then cooled from 423 to 298 K and finally re-heated to 423 K. The gray curves were collected during isothermal holdings at 423 and 298 K. Slow cooling and subsequent aging of the sample resulted in formation of a semicrystalline structure of the polymer matrix, containing amorphous phase and Form I crystals. As outlined in the discussion of Fig. 5, the mesophase did not completely convert to crystals, and consequently, the front X-ray scan contains weak peaks at  $11.8$  and  $18.4^\circ 2\theta$ , labeled II. Heating the semicrystalline structure to 423 K leads to melting of Form I crystals, with the subsequently detected X-ray pattern of the melt revealing LDH scattering at around  $11.7^\circ 2\theta$  (see arrow). Cooling of the melt leads to the formation of the Form II mesophase, which finally disorders without prior transformation to Form I crystals on re-heating.

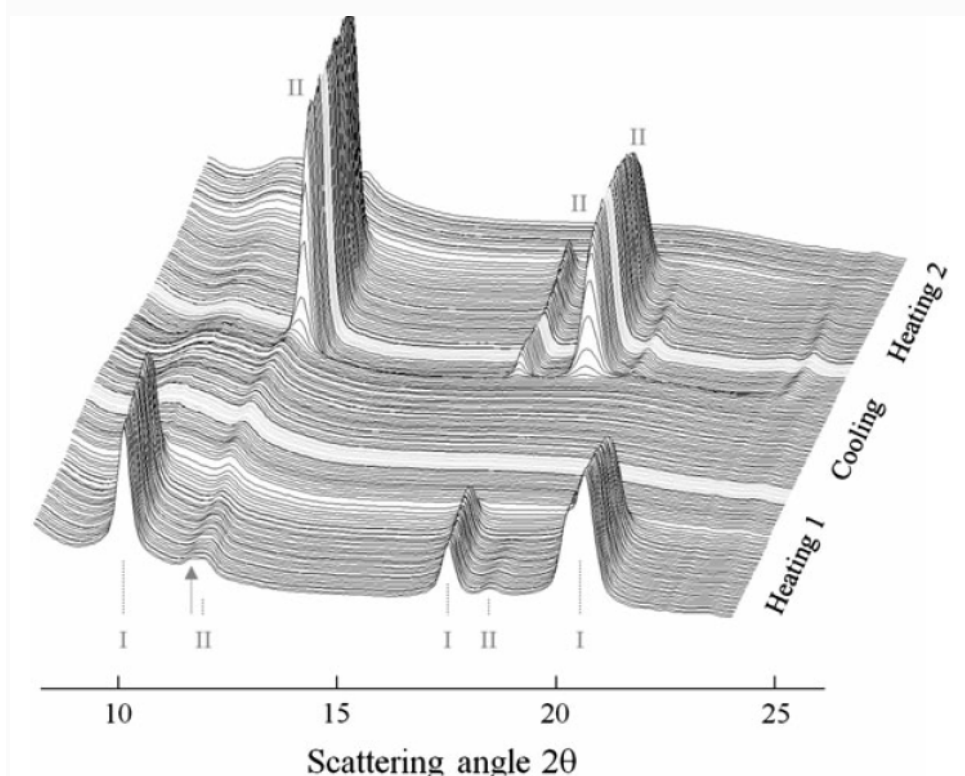


**Fig. 6** Series of WAXS curves, intensity as a function of scattering angle, of iPB-Eth/LDH-5, collected during heating, cooling, and reheating at rates of temperature change of  $5 \text{ K min}^{-1}$ . The *gray curves* indicate isothermal holding of the temperature at either 423 or 298 K, for periods of 3 min each. Data need to be read from *bottom to top*, with an increment of 2.5 K or 30 s between two subsequent curves

The data in Fig. 6 are representative for all investigated samples. Cooling the isotropic melt leads to formation of Form II mesophase which then on immediate heating disorders. In contrast, if the mesophase is kept at ambient temperature then it converts to Form I crystals. It has been found in the literature that the presence of nanofillers may affect the kinetics of the mesophase–crystal phase transition due to internal stress imposed on the mesophase [16–18, 21–23]. In order to prove/disprove such effect in the present case, we monitored the time-dependence of the mesophase–crystal phase transition.

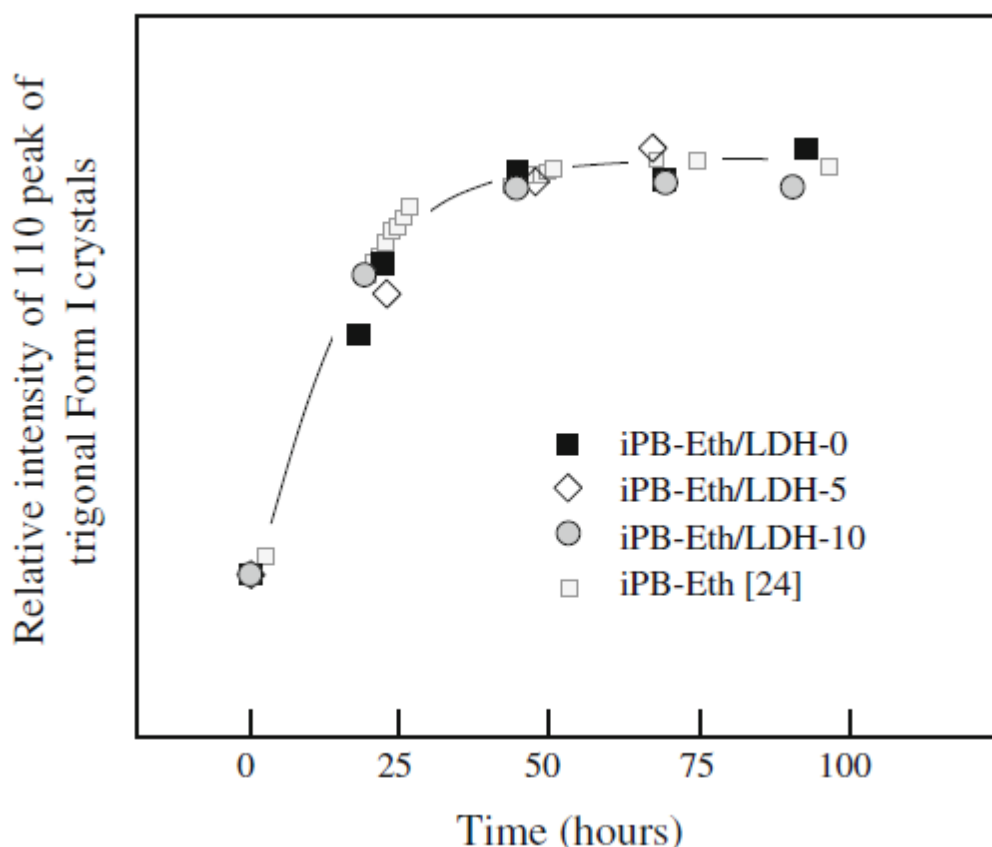


**Fig. 7.** Integral intensity of the WAXS 110 maximum at  $10.0^\circ 2\theta$  as a function of the annealing time at ambient temperature, representing the relative concentration of trigonal Form I crystals of the polymer matrix in the samples iPB-Eth/LDH-0 (*black squares*), iPB-Eth/LDH-5 (*diamond symbols*), and iPB-Eth/LDH-10 (*gray circles*), respectively. For comparison, the graph contains data collected in an earlier study about the crystal/mesophase polymorphism of the particular iPB-1 copolymer [24] (*gray squares*). Data were scaled to allow easy comparison of the Form II–Form I transition kinetics of the various samples

The samples were heated to 433 K, kept at this temperature for a period of 5 min to obtain a relaxed melt, cooled at a rate of  $2 \text{ K min}^{-1}$  to 298 K, and then aged at ambient temperature. During aging at ambient temperature, the unstable Form II mesophase which developed during cooling (see also Fig. 6) transformed to metastable Form I crystals. The kinetics of the mesophase–crystal transition was followed by monitoring the X-ray intensity of the 110 peak of Form I crystals of the polymer matrix as a function of the annealing time, shown in Fig. 7. The data reveal that the presence of LDH in the nanocomposites did not affect the mesophase–

crystal transition kinetics, and that the phase transition was completed after annealing for about 50 h in case of all samples of the present work. In Fig. 7, for the sake of statistics, we included additional data obtained on the same iPB-Eth copolymer collected in an independent study [24] (gray squares). An identical time-evolution of the relative crystal fraction during aging is revealed. The data in Fig. 7 suggest that the LDH nanofiller has a negligible effect on the local stress field, the structure, and defect concentration of the mesophase which, if different, perhaps would affect the transition kinetics. The obtained result is in accord with an independent study about the effect of presence of Perkalite LDH in iPB [18], as in this work even a slight delay of the phase transition was detected.

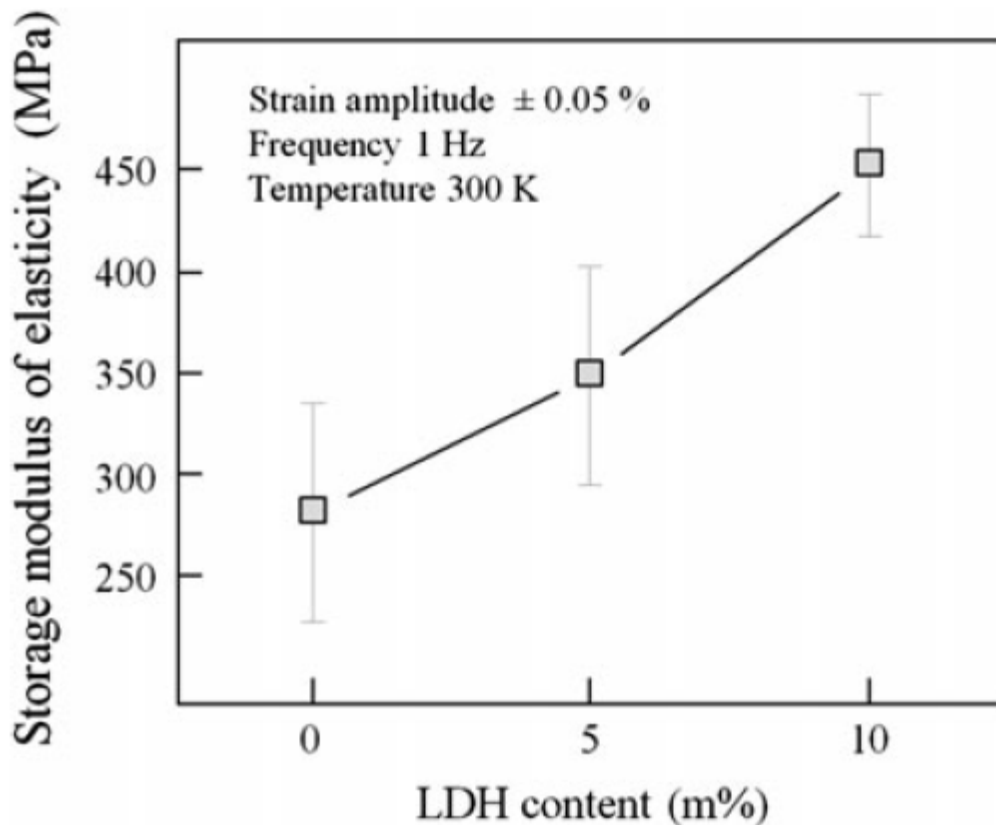


**Fig. 8.** Modulus of elasticity as a function of LDH content. The measurements were performed on aged samples, using DMA

A motivation of the present work was the use of LDH nanofillers to adjust the stiffness of the polymer. Acceleration of the disadvantageous mesophase–crystal phase transition of iPB, in order to obtain a stable material faster, can effectively be achieved by random copolymerization which, in general, is connected with a decrease of the crystallinity. The reduction of the crystallinity, in turn, leads to a lowering of the stiffness, and/or change of mechanical performance which may be compensated by addition of low amount of LDH nanofiller. In this initial work, we measured the modulus of elasticity to proof whether the approach suggested is applicable. In Fig. 8 the storage modulus of the various nanocomposites studied in this work is shown as a function of the concentration of the LDH nanofiller. For the unmodified copolymer, a value of 282 MPa was measured while the stiffness increased with increasing LDH content, to reach a value of 452 MPa at 10 m% LDH

loading. This result compares with an increase of the modulus of elasticity from 549 to 647 MPa on addition of 10 m% Perkalite LDH into the iPB homopolymer, reported recently [18]. As was discussed with Figs. 2, 3, 4, the LDH nanofiller leads to enhanced heterogeneous nucleation of the crystallization of the polymer matrix, which ultimately is connected with an increase of the number of spherulites; the beneficial effect of a fine-spherulitic morphology on mechanical properties including ductility or toughness has been described in detail in the literature [27].

## Conclusions

The present work was performed to demonstrate that the addition of LDH to iPB-1-based random copolymers provides an advantageous route to tailor the modulus of elasticity/stiffness. Random copolymerization of iPB-1 using 1-alkene co-units is an effective way to accelerate the disadvantageous mesophase–crystal transition after cooling the melt to ambient temperature. However, as this usually leads to decreases of the crystallinity and the perfection of crystals, the consequence is a loss of stiffness. It was shown with Fig. 8 that the modulus of elasticity of the specific butene-1-based random copolymer of this study containing 0.75 m% ethylene increased significantly from about 280 to 450 MPa on addition of 10 m% LDH, i.e., to a value reported for iPB-1 homopolymers [28]. In addition, the presence of LDH is connected with beneficial change of the semicrystalline superstructure of the polymer matrix. A distinct increase of the temperature of mesophase formation on cooling the melt is observed, that is, the LDH particles act as heterogeneous nucleation sites, accelerating the solidification process. As a result of the increased nucleation density, the size of spherulites in the polymer matrix is significantly decreased. The mesophase–crystal phase transition which follows the melt–mesophase transition on aging at ambient temperature, in contrast, is not affected by the presence of LDH. We speculate that the mesophase morphology at local scale, including size, surface structure and defect concentration is not largely affected by the addition of LDH.

## Acknowledgments

Financial support by the Deutsche Forschungsgemeinschaft (DFG, AN 212/11-1) and HasyLab/DESY is greatly acknowledged. We thank Chris van der Merwe and Antoinette Buys (University of Pretoria) for assistance in TEM analysis.

## References

1. Chatterjee AM (2008) Encyclopedia of polymer science and technology. Butene polymers
2. Luciani L, Seppälä J, Löfgren B (1988) Poly-1-butene: its preparation, properties and challenges. *Progr Polym Sci* 13:37–62
3. Danusso F, Gianotti G (1965) Isotactic polybutene-1: formation and transformation of modification 2. *Makromol Chem* 88:149–158
4. Boor J Jr, Mitchell JC (1963) Kinetics of crystallization and a crystal–crystal transition in poly-1-butene. *J Polym Sci Part A* 1:59–84

5. Azzurri F, Flores A, Alfonso GC, Balta Calleja FJ (2002) Polymorphism of isotactic poly(1-butene) as revealed by microindentation hardness. 1. Kinetics of the transformation. *Macromolecules* 35:9069–9073
6. Turner Jones A (1966) Cocrystallization in copolymers of  $\alpha$ -olefins II—butene-1 copolymers and polybutene type II/I crystal phase transition. *Polymer* 7:23–59
7. Gianotti G, Capizzi A (1969) Butene-1/propylene copolymers: influence of the comonomeric units on polymorphism. *Makromol Chem* 124:152–159
8. Azzurri F, Alfonso GC, Gomez MA, Marti MC, Ellis G, Marco C (2004) Polymorphic transformation in isotactic 1-butene/ethylene copolymers. *Macromolecules* 37:3755–3762
9. De Rosa C, Auriemma F, Vollaro P, Resconi L, Guidotti S, Camurati I (2011) Crystallization behavior of propylene–butene copolymers: the trigonal form of isotactic polypropylene and Form I of isotactic poly(1-butene). *Macromolecules* 44:540–549
10. Doyle MJ (2000) On the effect of crystallinity on the elastic properties of semicrystalline polyethylene. *Polym Eng Sci* 40:330–335
11. Halpin JC, Kardos JL (1976) Halpin-Tsai equations: a review. *Polym Eng Sci* 16:344–352
12. Halpin JC, Kardos JL (1972) Moduli of crystalline polymers employing composite theory. *J Appl Phys* 43:2235–2241
13. Kardos JL, Piccarolo S, Halpin JC (1978) Strength of discontinuous reinforced composites: II Isotropic crystalline polymers. *Polym Eng Sci* 18:505–511
14. Wanjale SD, Jog JP (2003) Poly(1-butene)/clay nanocomposites: preparation and properties. *J Polym Sci Part B* 41:1014–1021
15. Wanjale SD, Jog JP (2004) Poly(1-butene)/clay nanocomposites: a crystallization study. *J Macromol Sci Part B Phys* 43:1095–1114
16. Causin V, Marega C, Marigo A, Ferrara G, Idiyatullina G, Fantinel F (2006) Morphology, structure and properties of a poly(1-butene)/montmorillonite nanocomposite. *Polymer* 47:4773–4780
17. Marega C, Causin V, Marigo A, Saini R, Ferrara G (2010) Crystallization of a (1-butene)-ethylene copolymer in phase I directly from the melt in nanocomposites with montmorillonite. *J Nanosci Nanotech* 10:3078–3084
18. Marega C, Causin V, Neppalli R, Saini R, Ferrara G, Marigo A (2011) Effect of a synthetic double layer hydroxide on the rate of II  $\rightarrow$  I phase transformation of poly(1-butene). *eXPRESS. Polymer Lett* 5:1050–1061

19. Duan X, Evans DG (Volume Editors) (2006) Layered double hydroxides. Structure and Bonding, Mingos DMP (Series Editor), vol 119. Springer, Berlin
20. Leroux F, Besse JP (2001) Polymer interleaved layered double hydroxide: a new emerging class of nanocomposites. *Chem Mater* 13:3507–3515
21. Marega C, Causin V, Marigo A, Ferrara G, Tonnaer H (2009) Perkalite as an innovative filler for isotactic polypropylene-based nanocomposites. *J Nanosci Nanotech* 9:2704–2714
22. Goldbach G (1973) Zur Umwandlung der polymorphen Struktur von Polybuten-1 unter der Wirkung mechanischer Spannungen. *Angew Makromol Chem* 29(30):213–227
23. Nakafuku C, Miyaki T (1983) Effect of pressure on the melting and crystallization behaviour of isotactic polybutene-1. *Polymer* 24:141–148
24. Nase M, Androsch R, Langer B, Baumann HJ, Grellmann W (2008) Effect of polymorphism of isotactic polybutene-1 on peel behavior of polyethylene/polybutene-1 peel systems. *J Appl Polym Sci* 107:3111–3118
25. Wunderlich B (2005) Thermal analysis of polymeric materials. Springer, Berlin
26. Androsch R, Di Lorenzo ML, Schick C, Wunderlich B (2010) Mesophases in polyethylene, polypropylene, and poly(1-butene). *Polymer* 51:4639–4662
27. Weynant E, Haudin JM, G'Sell C (1980) In situ observation of the spherulite deformation in polybutene-1 (Modification I). *J Mater Sci* 15:2677–2692
28. Polybutene-1 product information, LyondellBasell. <https://polymers.lyondellbasell.com>